Size Effect on the Shear Strength of High-Strength Concrete Continuous Beams Reinforced with GFRP Bars

Karam Mahmoud[1] and Ehab El-Salakawy[2]

[1] Ph.D. Candidate, Dept. of Civil Eng., University of Manitoba, Winnipeg, MB, Canada
[2] Professor and CRC, Dept. of Civil Eng., University of Manitoba, Winnipeg, MB, Canada

Abstract: The use of the non-corrodible fiber reinforced polymer (FRP) bars as main reinforcement for concrete structures to overcome the steel corrosion problem is exponentially increasing. Compared to steel reinforcement, the use of FRP bars, as beam longitudinal reinforcement, resulted in more pronounced size effect on shear strength. This effect was more significant in beams made of high strength concrete and with small longitudinal reinforcement ratio. This study evaluates the size effect on shear capacity of continuous high-strength concrete beams reinforced with glass (G) FRP bars. The experimental results of six large-scale continuous concrete beams are presented. The test beams had a rectangular cross section of 200 mm width and three different effective depths of 250, 500 and 750 mm. The beams were continuously supported over two equal spans of 2,800, 3,750 and 5,250 mm for beams with depth of 250, 500 and 750 mm, respectively. The test variables were the effective depth of the beam and the longitudinal reinforcement ratio. The test results showed that significant size effect was observed with increasing the effective depth in beams failed in the exterior shear span. On the other hand, in beams failed in the interior shear span, no size effect was observed.

1 Introduction

The size effect on shear strength of steel-reinforced concrete (RC) beams has been always a major concern as it was reported that the shear stress at failure decreased as the member depth increased (Kani 1967, Shioya et al. 1989, Bažant and Kim 1984, Collins & Kuchma 1999 and Bentz 2005). This effect is more sever in the case of large members made of high strength concrete (HSC) beams Collins and Kuchma (1999). Most of the current codes for steel-RC structures account for such effect. Similarly, recent research conducted to study the size effect on shear strength on simply-supported beams reinforced with FRP bars showed the use of FRP bars, as longitudinal reinforcement, led to a more pronounced size effect than that in steel-RC beams when either normal strength or high strength concrete is used (Alam and Hussein 2012 and 2013). Also, Bentz et al. (2010) concluded that the same size and strain effects on the shear strength in steel-RC beams were observed in FRP-RC beams.

The shear behaviour of continuous beams reinforced with steel bars has been widely investigated. It was found that because of the established moment and shear redistribution in such members, the diagonal tension cracking analysis used in simple beams can be applied to continuous beams (Ernst1958; Rodrigues et al. 1959; Bryant et al. 1962). Moreover, the size effect on steel-RC continuous beams was investigated by Collins and Kuchma (1999). It was reported that the shear stress at failure decreased with increasing the member size. Also, the decrease in the shear strength of beams made of HSC was slightly greater than that in NSC beams.

On the other hand, for FRP-RC continuous beams, it was reported that moment redistribution occurred (Razaqpur and Mostofinejad 1999; Habeeb and Ashour 2008; Gravina and Smith 2008). Following this effort, an extensive research program has started at the University of Manitoba to study the behavior of concrete continuous beams reinforced with FRP bars (El-Mogy et al. 2010 & 2011; Mahmoud and El-Salakawy 2014). In addition, up to authors' knowledge, there is no research data available on

investigating the size effect on the shear strength of continuous concrete beams reinforced with FRP bars. Therefore, this paper represents the first attempt to understand the size effect on the shear strength of GFRP-RC continuous beams and to examine if the current design equations can predict safely the shear strength of such beams.

2 EXPERIMENTAL PROGRAM

Six large-scale, two-span continuous HSC beams reinforced with GFRP bars and without shear reinforcement were constructed and tested to failure. The variables were the effective depth of the beam and longitudinal reinforcement ratio (0.8% and 1.2%). The test beams had a rectangular cross section of 200 mm width and three different effective depths of 250, 500 and 750 mm. All test beams were designed to fail in shear and the longitudinal reinforcement was arranged to satisfy 20% moment redistribution from the hogging to the sagging regions. The specimen designation can be explained as follows. The letter "G" refers to GFRP bars as reinforcing materials while "H" refers to the concrete grade, HSC. The number is for the longitudinal reinforcement ratio and the last letter refers to refers to the size of the beam where "S" for small size beams with 250 mm depth, "M" for medium size beams with 500 mm depth and "L" for large size beams with 750 mm depth. Details of the test specimens are shown in Fig. 1 and Table 1.

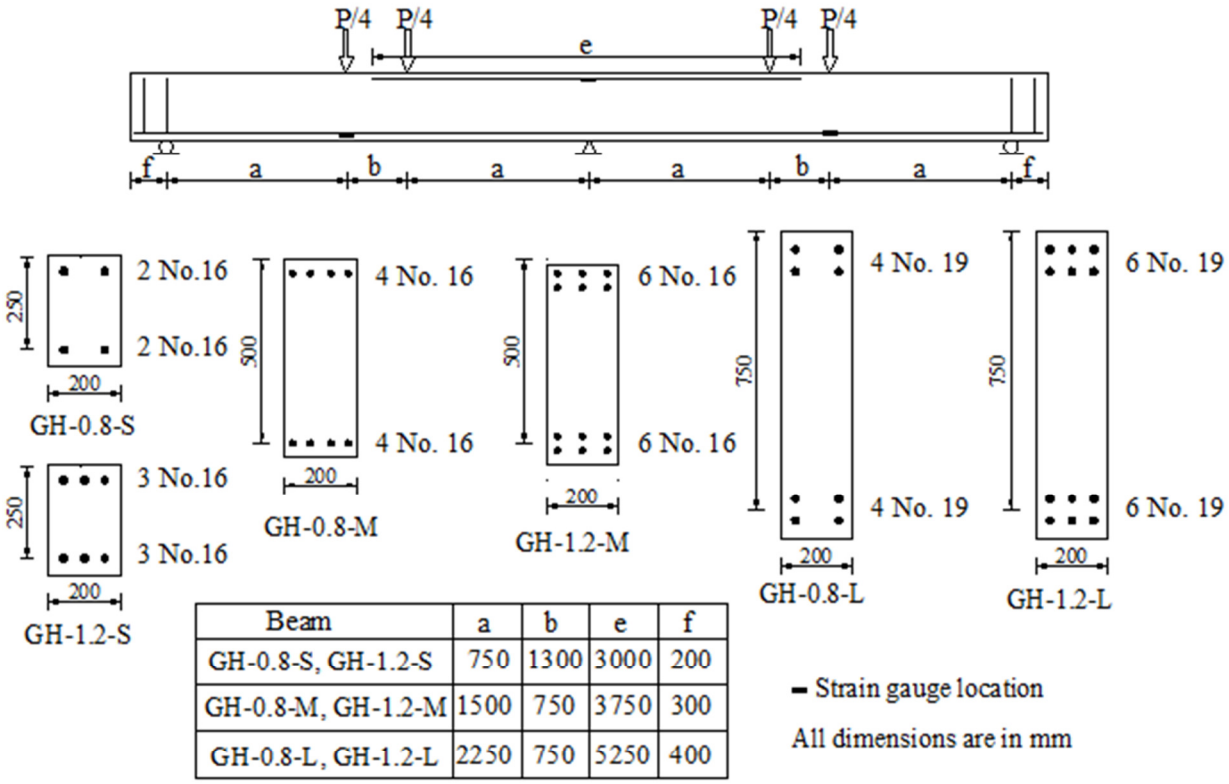

Beam	a	b	e	f
GH-0.8-S, GH-1.2-S	750	1300	3000	200
GH-0.8-M, GH-1.2-M	1500	750	3750	300
GH-0.8-L, GH-1.2-L	2250	750	5250	400

Figure 1: Details and internal instrumentation of test beams

Table1 – Concrete strength and reinforcement details of test specimens

Beam	f_c' MPa	Longitudinal reinforcement, top and bottom		
		ρ (%)	Details of reinforcement	Reinforcement rigidity, $E_r\rho_r$, (MPa)
GH-0.8-S	72	0.79	2 No.16	536
GH-0.8-M	70	0.79	4 No.16	536
GH-0.8-L	77	0.76	4 No.19	496
GH-1.2-S	72	1.18	3 No.16	799
GH-1.2-M	70	1.18	6 No.16	799
GH-1.2-L	77	1.14	6 No.19	744

2.1 Test Setup and Instrumentation

All test beams were supported on two roller supports at both ends and one hinged support at the middle. The beams were tested under two-point loading system in each span with a constant shear span-to-depth ratio of 3.0. For the small size beams (250 mm depth), a 1000-kN MTS machine was used to apply monotonic concentrated loading through a system of rigid steel spreader beams. For larger size beams (500 and 750 mm depth), the MTS machine and a 1000-kN MTS hydraulic actuator were used to apply the load to the beam. A load-controlled rate of 10 kN/min was used to apply equal loads to the two spans. The load was occasionally paused for visual inspection of the beam and marking the cracks. Readings of all instrumentations and load cells were collected using a data acquisition system and stored on a personal computer.

Two load cells were used to measure the reactions at the two exterior supports. Moreover, deflection was measured, using linear variable differential transformers (LVDTs), at three different locations in each span, at mid-span and at each loading point in the span. The strains in both longitudinal reinforcement and concrete were measured at three critical sections, over the middle support and under the exterior load in each span. Details of instrumentations are shown in Figs. 1 and 2.

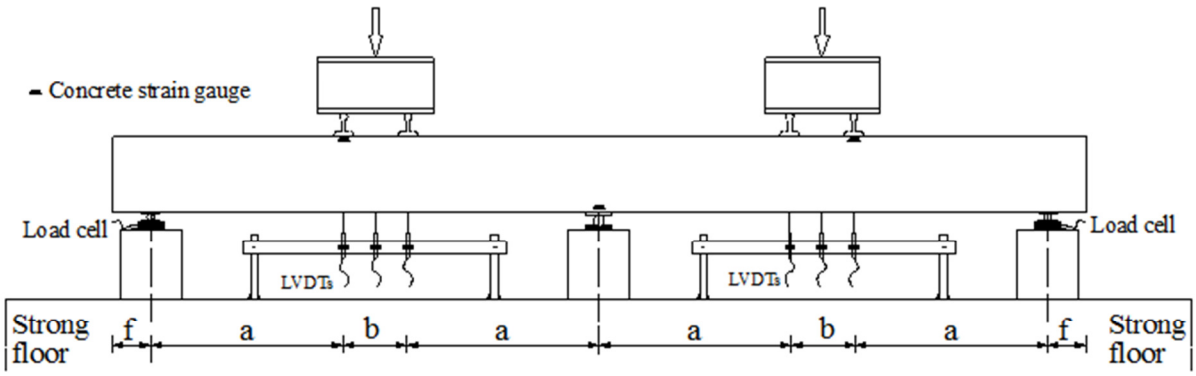

Figure 2: Test setup and external instrumentations of test beams

2.2 Materials

Sand-coated GFRP bars were used as longitudinal and transverse reinforcement. The properties of the used bars are given in Table 1. All beams were cast from a ready-mixed concrete with a target 28-day concrete strength of 70 MPa. The average concrete strength for different beams, obtained on the day of beam testing, is listed in Table 2.

Table 2 – Properties of reinforcing GFRP bars

Bar size	Nominal Area (mm2)	Tensile strength (MPa)	Modulus of Elasticity (GPa)	Ultimate strain (%)
No.16	197.8	1440	67.7	2.1
No.19	285.0	1480	65.3	2.3

3 TEST RESULTS AND DISCUSSION

3.1 Mode of Failure and Cracking Pattern

All tested beams failed in shear due to a diagonal tension crack formed in the interior shear span, in the exterior shear span or simultaneously in both shear spans. Beams GH-0.8-S, GH-1.2-S and GH-1.2-L failed in the interior shear span, near the middle support. On the other hand, beams GH-0.8-M and GH-0.8-L in the exterior shear span. The failure of beam GH-1.2-M was due to two diagonal tension cracks, one was in the interior shear span while the other one was in the exterior shear span. Figure 3 shows schematic drawings of the cracking pattern of all test beams at failure. It can be seen that, in beams with 250 mm depth (GH-0.8-S and GH-1.2-S), the majority of cracks were vertical flexural cracks concentrated in the maximum moment regions (over the middle support and under the exterior loading points). Also, there were few diagonal cracks formed near failure of the beams. Similar cracking pattern was observed in medium and large size beams (GH-0.8-M, GH-1.2-M, GH-0.8-L and GH-1.2-L); however, flexural cracks formed near the interior loading point and diagonal cracks were observed in the interior shear spans. Also, as the effective depth increases, secondary flexural cracks were formed in both the hogging and sagging moment regions. Furthermore, with increasing the effective depth, the cracking pattern became similar to that of a simply-supported beam where more flexural and diagonal cracks were observed near the interior loading point.

3.2 Deflection

Figure 4 shows the load-deflection relationship at mid-span of all test beams in the span where failure took place. Generally, the typical load-deflection curve can be divided, similar to simply-supported beams, into two distinct stages, pre-cracking and post-cracking. In the pre-cracking stage, the measured deflection was insignificant in all beams; however, the deflection increased after the formation of the first flexural crack in the beam. At the beginning of the post-cracking stage, the initiation of more cracks resulted in a decrease in the flexural stiffness of the beams; then, the behavior of the beams became almost linear until failure. It can be seen that the size of the beam did not affect significantly the slope of the load-deflection relationship in the post-cracking stage which was very similar for beams having approximately the same longitudinal reinforcement ratio, until failure. As expected, increasing the longitudinal reinforcement ratio/rigidity increased the post-cracking flexural stiffness.

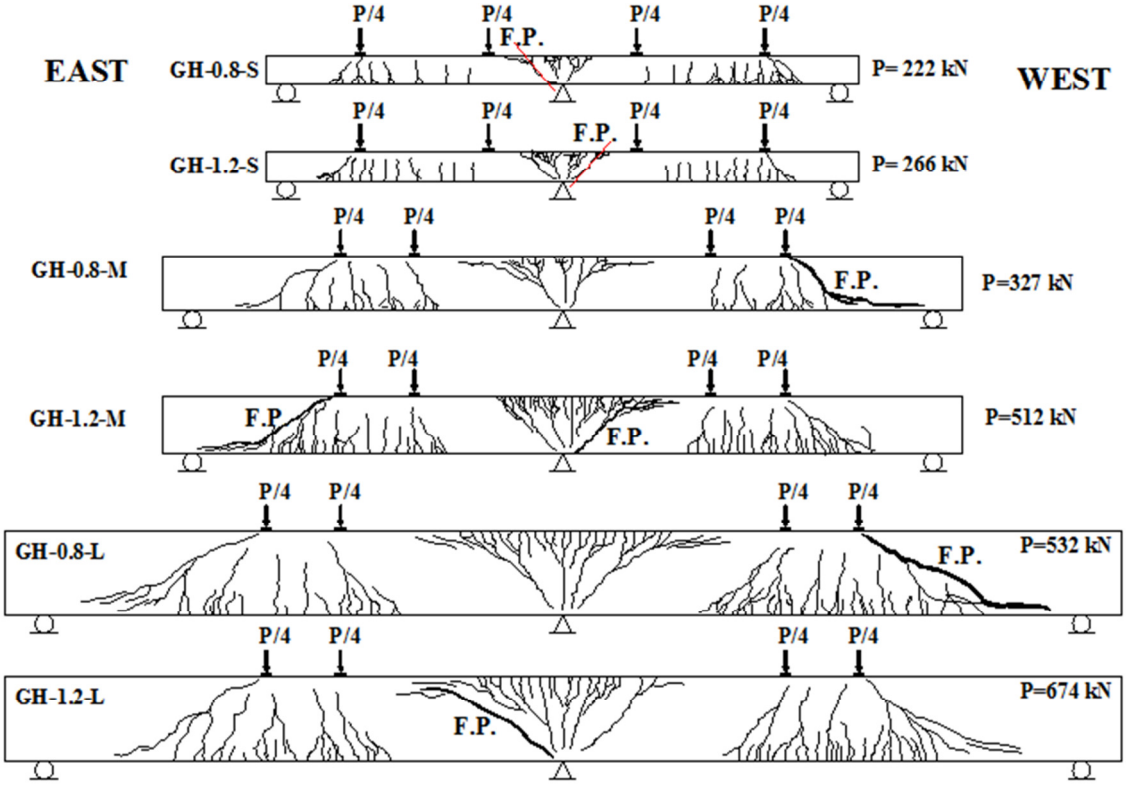

Figure 3: Cracking pattern at failure of test beams

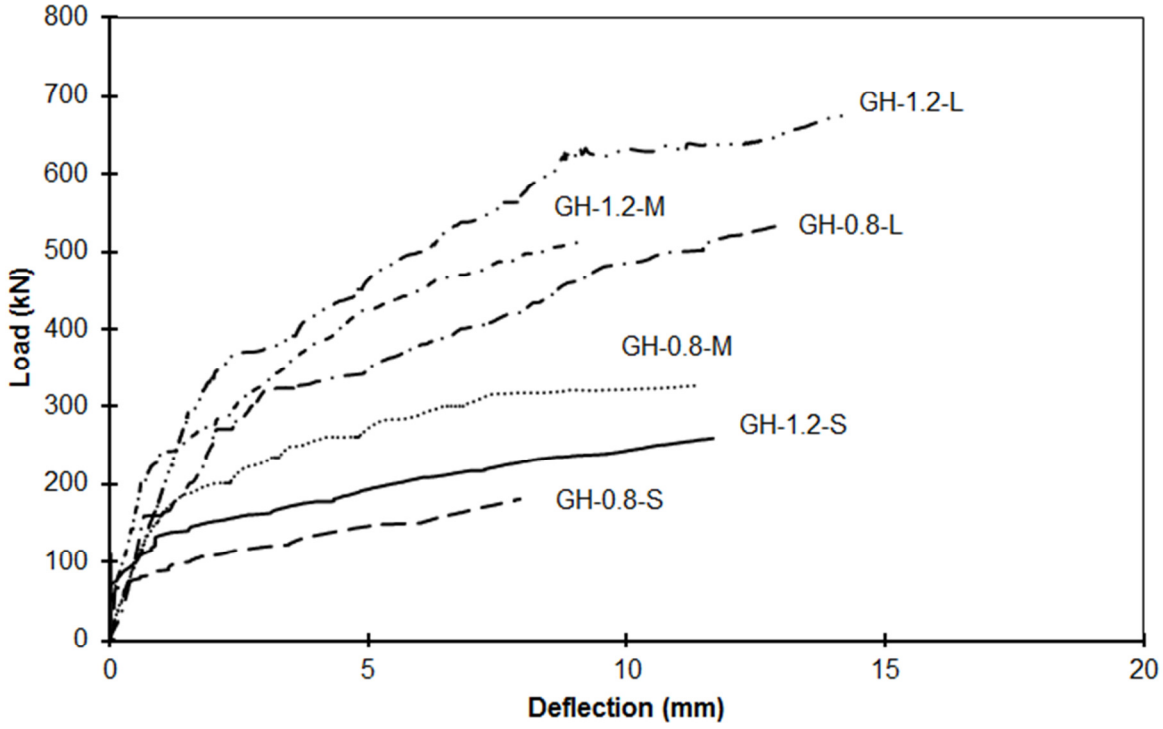

Figure 4: Load-deflection relationship at mid-span of test beams

3.3 Reactions and Moment Redistribution

The measured exterior reactions were used to calculate the shear force and bending moment distribution along the beam. The moment redistribution is then calculated based on the actual and theoretical bending moment at failure. In beams having 250 and 500-mm depth, the exterior reaction followed the elastic distribution at early stages of loading. After the formation of flexural cracks at the middle support region, the measured end reactions started to have higher values than those obtained by the elastic theory. This trend continued until failure of the beam as can be seen in Fig. 5. Higher exterior reactions than the elastic ones means normal redistribution of bending moment occurred from hogging to sagging moment regions. The percentage of moment redistribution in beams GH-0.8-S, GH-0.8-M, GH-1.2-S and GH-1.2-M, from hogging to sagging moment regions, was approximately 20.8%, 17.4%, 16.7% and 11.0%, respectively. This behavior agrees well with the findings of the recent research conducted on continuous beams reinforced with FRP bars (Kara and Ashour 2013 and El-Mogy et al. 2010 & 2011).

On the other hand, large size beams GH-0.8-L and GH-1.2-L, showed significantly different behavior where the exterior reactions deviated from the elastic distribution but, this time, they were of smaller values compared to those calculated by the elastic theory. This behaviour continued until the failure of the beams resulting in reversed moment redistribution from sagging to hogging moment regions. The percentage of moment redistribution at failure was -17.0% and -14.3% in beams GH-0.8-L and GH-1.2-L, respectively. The reversed moment redistribution in these beams can be attributed to the extensive flexural cracking in the sagging moment regions while no more cracks formed in the hogging moment region in these beams (GH-0.8-L and GH-1.2-L).

It can be noted that increasing the beam depth changed the magnitude and direction of moment redistribution. The moment redistribution reached 20.8 % in beam GH-0.8-S, decreased slightly to 17.4% in beam GH-0.8-M, and then decreased dramatically to -17% in beam GH-0.8-L. Similarly, the moment redistribution was 16.7%, 11.0% and -14.3% in beams GH-1.2-S, GH-1.2-M and GH-1.2-L, respectively. As discussed above, this could be attributed to the wider and additional cracks developed in the sagging moment regions compared to those in the hogging moment region. This resulted in a relatively weaker sagging moment region which caused the internal forces redirected to the relatively stronger zone (the hogging moment zone).

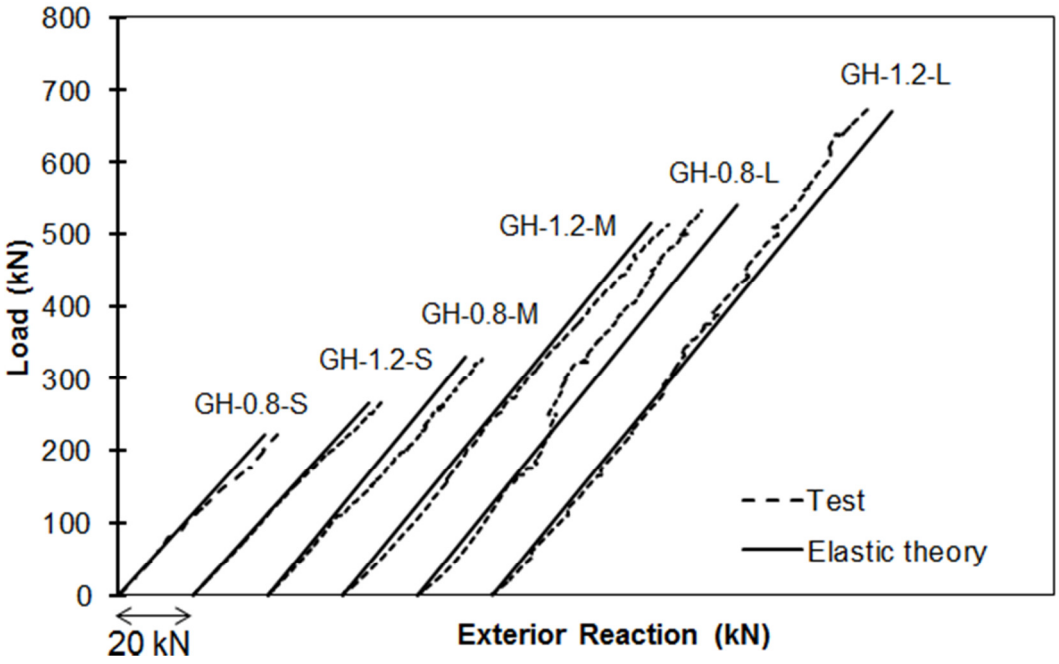

Figure 5: Load-exterior reaction relationship of test beams

3.4 Shear Strength

The experimental shear stress and normalized shear stress at failure in both interior and exterior shear spans are shown in Fig. 6 and listed in Table 3. It can be noted that beams failed in the interior shear span exhibited no size effect where the shear strength increased as the effective depth increased. In HSC beams with longitudinal reinforcement ratio of 1.2%, there is no significant change in the shear strength where beams having 250, 500 and 750 mm failed at approximately the same shear stress. However, this behavior is still contradicting the well-established size effect in simply-supported beams especially that the size effect is more pronounced in HSC beams. On the other hand, the shear strength of the test beams failed in the exterior shear span was strongly affected by the size of the beam. It can be noted that increasing the depth from 500 mm in beam GH-0.8-M to 750 mm in GH-0.8-L resulted in a decrease in the shear strength at the exterior shear span by 13% (from 0.56 to 0.49 MPa) as well. Regardless of the failure location in the test beams, the shear strength decreased with increasing the depth at the exterior shear span in beams having longitudinal reinforcement ratio of 0.8% and 1.2%. This decrease was greater in the case of beams with longitudinal reinforcement ratio 0.8%. This can be attributed to the width of the diagonal crack where it was observed that the diagonal cracks in the exterior shear span were wider than those in the interior shear span.

To investigate the continuity effect on the different size beams, test results were compared to simply-supported GFRP-RC beams reported in literature. Bentz et al. (2010) tested six simple beams without shear reinforcement. Three beams had a longitudinal reinforcement ratio in the range of 0.5 to 0.66 % and a depth in the range of 194 to 938 mm. It was found that increasing the depth from 194 to 438 mm resulted in a reduction of the normalized shear strength by 29% while increasing the depth from 438 to 938 mm resulted in a decrease of 37% in the normalized shear strength. The other three beams had a higher longitudinal reinforcement ratio (ranged from 2.23 to 2.54%) demonstrated lower decrease in the shear strength when the depth increased. Increasing the depth from 188 to 405 mm and from 405 to 860 mm resulted in a decrease in the shear strength by 14 and 22%, respectively. Matta et al. (2013) tested beams having depths of 292 and 883 mm. It was reported that the shear strength, in beams having 0.59% longitudinal reinforcement ratio, reduced by 30% when the depth increased from 292 mm to 883 mm (11.5 to 34.76 in.). Alam and Hussien (2012 & 2013) reported similar decrease in the shear strength (20%) when the depth increased from 291 to 578 mm in NSC beams with a reinforcement ratio ranging from 0.86 to 0.91%. Higher reduction in the shear strength (38%) occurred when the depth increased from 305 to 734 mm (12 to 28.9 in.) in HSC beams with a reinforcement ratio ranging from 0.87 to 1.37%.

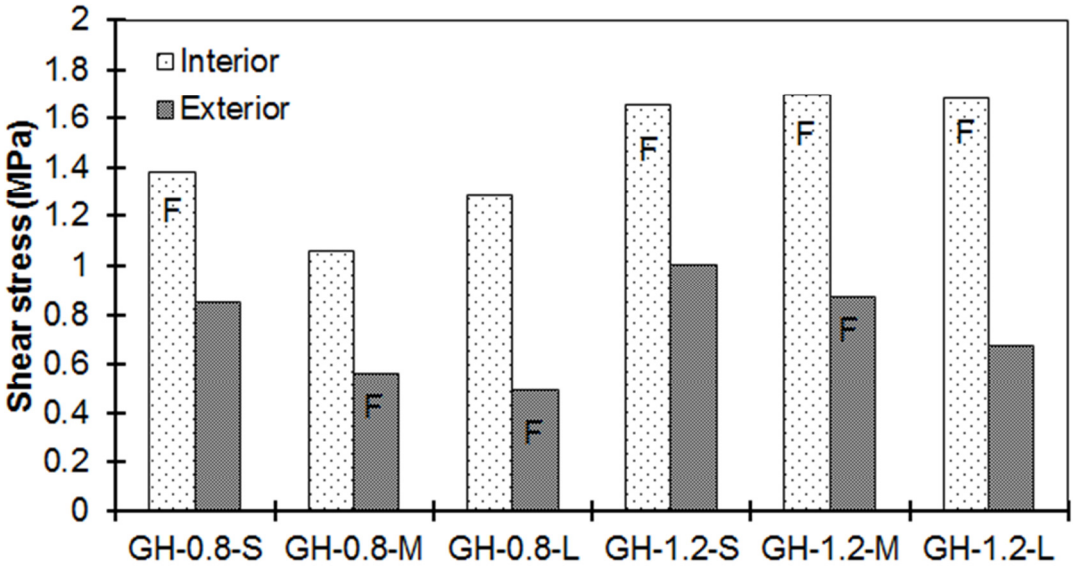

Figure 6: Shear strength of tested beams at interior and exterior shear span (F = failure)

Table 3 – Shear strength and normalized shear strength of test beams

Beam	Shear strength, $v_{test,}$ (MPa)		$\frac{V_{test}}{\sqrt{f_c'}\, b_w d}(\sqrt{MPa})$	
	Int.	Ext.	Int.	Ext.
GH-0.8-S	1.38*	0.85	0.162	0.100
GH-0.8-M	1.06	0.56†	0.127	0.067
GH-0.8-L	1.28	0.49†	0.146	0.056
GH-1.2-S	1.66*	1.00	0.196	0.118
GH-1.2-M	1.70*	0.87†	0.203	0.104
GH-1.2-L	1.68*	0.67	0.191	0.076

* shear strength in the interior shear span at failure,
† shear strength in the exterior shear span at failure,

4 CONCLUSIONS

Six GFRP-RC continuous beams were tested to failure. Based on the test results presented and discussed above, the following conclusions can be drawn.

1. The moment redistribution, from the hogging to the sagging moment regions, decreased or changed direction (form the sagging to the hogging moment region) with increasing the effective depth. This could be attributed to the wider and additional cracks developed in the sagging moment regions compared to those in the hogging moment region. This resulted in a relatively weaker sagging moment region which caused the internal forces redirected to the relatively stronger zone (the hogging moment zone).

2. GFRP-RC continuous beams failed in the interior shear span showed no size effect on the shear strength of such beams. The shear strength of HSC beams approximately did not change as the effective depth increase.

3. Similar to simply-supported beams, size effect on the shear strength of was observed in beams failed in the exterior shear span where the shear strength decreased significantly as the effective depth increased.

5 ACKNOWLEDGMENTS

The authors wish to express their sincere appreciation to the Natural Sciences and Engineering Research Council of Canada (NSERC) through the Canada Research Chairs Program. The assistance received from the technical staff of the MaQuade structures laboratory at the University of Manitoba is acknowledged.

6 REFERENCES

ACI Committee 440. (2006). “Guide for the Design and Construction of Structural Concrete Reinforced with FRP Bars.” *ACI 440.1R-06*, Detroit.

Alam, M. and Hussein, A. (2012). “Effect of member depth on shear strength of high-strength fiber-reinforced polymer-reinforced concrete beams.” *J. Compos. Constr.* 10-1061/(ASCE) CC.1943-5614.0000248, 119-126.

Alam, M. and Hussein, A. (2013). “Size effect on shear strength of FRP reinforced concrete beams without stirrups.” *J. Compos. Constr.*, 10.1061/(ASCE)CC.1943-5614.0000346, 507- 516.

Bažant, Z. P., and Kim, J. (1984). “Size effect in shear failure of longitudinally reinforced beams.” *ACI Struct. J.*, 81(5), 456–468.

Bentz, E. C. (2005). “Empirical modeling of reinforced concrete shear strength size effect for members without stirrups.” *ACI Struct. J.*, 102(2), 232-241.

Bentz, E., Massam, L. and Collins, M. (2010). “Shear strength of large concrete members with FRP reinforcement.” *J. Comp. Constr., ASCE*, 15(6), 637-646.

Bryant, R., Bianchini, A., Rodriguez, J. and Kesler, C. (1962). “Shear strength of two-span continuous reinforced concrete beams with multiple point loading.” *ACI Struct. J.*, 59(9), 1143-1177.

Canadian Standard Association (CSA). (2012). “Code for the design and construction of building structures with fibre-reinforced polymers” *CAN/CSA-S806-12*, Canadian Standard Association, Rexdale, ON, Canada.

Collins, M. P. and Kuchma, D. (1999). “How safe are our large, lightly reinforced concrete beams, slabs, and footings?” *ACI Struct. J.*, 96(4), 482-491.

El-Mogy, M., El-Ragaby, A. and El-Salakawy, E. (2010). “Flexural behavior of continuous FRP-reinforced concrete beams.” *J. Comp. Constr.*, 10.1061/(ASCE)CC.1943-5614.0000140, 669-680.

El-Mogy, M., El-Ragaby, A. and El-Salakawy, E. (2011). “Effect of transverse reinforcement on the flexural behavior of continuous concrete beams reinforced with FRP.” *J. Comp. Constr.*, 10.1061/(ASCE)CC.1943-5614.0000215, 672-681.

Ernst, G. C. (1958). “Moment and shear redistribution in two-span continuous reinforced concrete beams.” *ACI Struct. J.*, 30(5), 573-589.

Gravina, R. J. and Smith, S. T. (2008). “Flexural behaviour of indeterminate concrete beams reinforced with FRP bars.” *Eng. Struct.*, 30(9), 2370–2380.

Habeeb, M. N. and Ashour, A. F. (2008). “Flexural behavior of continuous GFRP reinforced concrete beams.” *J. Compos. Constr.,* 10.1061/(ASCE)1090-0268(2008)12:2(115), 115–124.

Kani, G. N. J. (1967). “How safe are our large concrete beams?” *ACI J. Proc.*, 64(3), 128–141.

Mahmoud, K. and El-Salakawy, E. (2014). “Shear strength of GFRP-reinforced concrete continuous beams with minimum transverse reinforcement.” *J. Compos. Constr.*, 10.1061/(ASCE)CC.1943-5614.0000406, 04013018.

Matta, F., El-Sayed, A., Nanni, A. and Benmokrane, B. (2013). “Size effect on concrete shear strength in beams reinforced with fiber-reinforced polymer bars.” *ACI Struct. J.*, 110 (4), 617-628.

Mattock, A. H. (1959). “Redistribution of design bending moments in reinforced concrete continuous beams” *ICE Proc.*, 13(1), 35-46.

Razaqpur, G.A. and Mostofinejad, D. (1999). “Experimental study of shear behavior of continuous beams reinforced with carbon fiber reinforced polymer.” *4th Intl Symp. Fiber Reinforced Polymer Reinforcement for Reinforced Concrete Structures, SP188-16*, ACI, Detroit, 169-178.

Shioya, T., Iguro, M., Nojiri, Y., Akiyama, H. and Okada, T. (1989). “Shear strength of large reinforced concrete beams, fracture mechanics: Application to concrete.” *SP-118*, ACI, Detroit, MI, 259-279.